Chapter 7

Printed Wide Slot Ultra-Wideband Antenna

Rezaul Azim and Mohammad Tariqul Islam

Additional information is available at the end of the chapter

http://dx.doi.org/10.5772/51961

1. Introduction

With the beginning of the new information era, necessity of wideband wireless communications technology is increasing rapidly due to the need to support more users and to provide information with higher data transmitting rates. Ultra-wideband (UWB) technology could be the most suitable technologies that promise to revolutionize high data rate transmission and enable the personal area networking industry leading to new innovations and greater quality of services to the end users. A UWB system is found to be extremely useful and consists of various satisfying features such as high data rate, high precision ranging, fading robustness, and low cost transceiver implementation. UWB is regarded as a very promising and fast emerging low-cost technology with uniquely attractive features inviting major advances in wireless communications, sensor networking, radar, imaging, and positioning systems [1, 2].

Antennas are indispensable elements of any wireless communication systems. For UWB communication systems, the antennas must be of low profile, compact size, light weight, low cost and conformable to the architecture of the mounting devices. Amongst various types of antennas such as log periodic, TEM horn, stacked patch, spiral and planar structure, the antenna with planar profile seems to be the most preferred choice [3-5]. It has the advantage of low profile in size, compactness, and easily embeddable into wireless devices or integratable with other RF circuitry

In recent years, printed slot antennas are under consideration for use in UWB applications and are getting more and more popular because of the merits of wide frequency bandwidth, low profile, lightweight, ease of fabrication and integration with other devices or RF circuitries. Compared to the electrical antennas, slot antennas have relatively large magnetic fields that tend not to couple strongly with near-by objects, which make them suitable for applications wherein near-filed coupling is required to be minimized [6]. A conventional narrow

slot antenna has limited bandwidth, whereas wide-slot antennas exhibit wider bandwidth. Recently, different printed wide-slot antennas fed by a microstrip line or coplanar waveguide have been reported [7, 8]. Apart from these antennas, monopole like slot antennas have also been reported to have wide bandwidth characteristics [9-11]. By using different tuning techniques or employing different slot shapes such as rectangle, circle, arc-shape, annular-ring, U-shaped [12-16], different slot antennas achieved wideband or ultra-wideband performance. A square slot antenna excited by a CPW-fed widened tuning stub was proposed in [17]. By properly choosing the location and size of the tuning stub, the proposed antenna achieved a bandwidth of 60% with an overall dimension of 72 mm × 72 mm. In [18], a novel broadband design of a CPW-fed square slot antenna loaded with conducting strips has been introduced. The -10 dB impedance bandwidth of the proposed slot antenna is more than 60%. In [19], a printed wide-slot antenna fed by a microstrip line is introduced. By employing an arc-shaped slot and a square-patch feed, the antenna achieved an impedance bandwidth ranging from 1.82 GHz to 7.23 GHz. Although the antenna achieved a good impedance bandwidth with an overall dimension of 110 mm × 110 mm, it does not operate within the entire UWB. The design of a printed wide-slot antenna with a rotated slot is presented in [20]. The impedance bandwidth of the antenna varies with the rotation angle of the slot and can maintain 50.2% with suitable angle. More recently, the design of a printed wide-slot antenna for wideband applications is proposed in [21]. The antenna consists of an E-shaped patch and E-shaped slot and achieves an impedance bandwidth of 120% (2.8 - 11.4 GHz). However, the antenna does not possess a compact profile having a dimension of 85 mm × 85 mm. A new CPW-fed tapered ring slot antenna was presented in [22]. With an overall size of 66.1 mm × 44 mm, the proposed antenna achieved an impedance bandwidth range of 8.9 GHz (ranging from 3.1 - 12 GHz). The actual bandwidth was, however, limited by the distortion of radiation patterns.

In this chapter, a printed wide slot antenna that achieves a physically compact planar profile having sufficient impedance bandwidth and omnidirectional radiation pattern is proposed for UWB communication systems. By etching a microstrip fed rectangular tuning stub as radiating element and a tapered shape slot in the ground plane, the proposed antenna achieved a UWB characteristics. The antenna structure is flat, and its design is simple and easy to fabricate.

2. Antenna configuration

The geometry and configuration of the proposed antenna is illustrated in Figure 1. The antenna consists of a tapered shape slot etched out of the ground plane and a microstrip line fed rectangular tuning stub for excitation. The tuning stub fed by microstrip line of 50 Ω characteristics impedance is printed on one side of an inexpensive FR4 substrate of thickness 1.6 mm, with relative permittivity 4.6 and loss tangent 0.02 while the slot is etched out on the other side. The reason for choosing FR4 substrate material is its low cost. Despite of relatively high loss tangent, the antenna fabricated on FR4 achieved moderate gain and efficient, which are sufficient for UWB wireless communications. The slot in the ground plane con-

sists of two sections: the rectangular section of dimension $W_3 \times L_1$ and the triangular section, which is tapered with a slant angle $\alpha = 90^0$ for a length L_2 and has strong coupling to the feeding structure. The distance between bottom edge of the tuning stub and lower edge of the tapered shape slot is h. Therefore by properly selecting the slot shape and tuning stub, a good impedance bandwidth and radiation characteristics can be achieved. The overall size of the proposed antenna is only 22 mm × 24 mm, which can be considered as one of the smallest UWB slot antenna found in open literature.

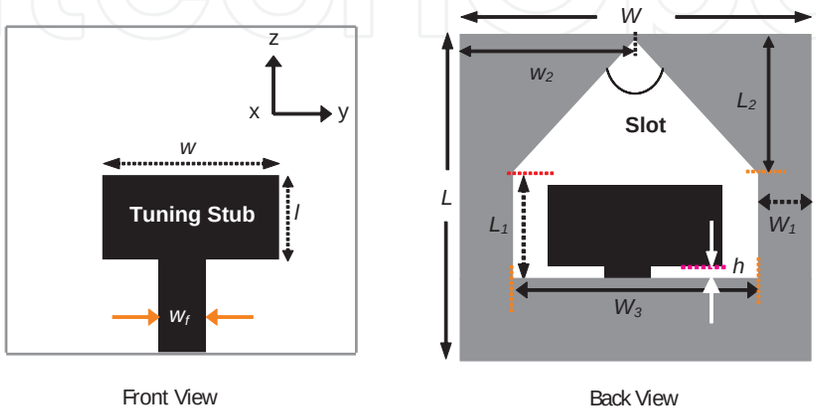

Figure 1. Geometry and detailed view of the proposed slot antenna.

3. Effects of designed parameters

Based on this design, some sensitive parameters are studied numerically in order to investigate the influence of the parameters on antenna performance. In the simulation only one parameter was varied each time, where as the others were kept constant. All simulation was carried out by employing Zeland's IE3D based on method of moment [23].

3.1. Effect of the tuning stub

Usually a large slot is used in a wide-slot antenna to achieve a high level of electromagnetic coupling to the tuning stub. Therefore variation of the tuning stub shape and slot shape will change the coupling; and thus control the impedance matching. In order to optimize the coupling between the microstrip-line and the tapered slot, different stub shapes are studied. The rectangular shape tuning stub is compared with four other stubs as shown in Figure 2. Figure 3 shows the simulated return loss curves for the five different stubs. It is observed that, for elliptical and circular shape tuning stubs, the impedance matching become very poor due to poor electromagnetic coupling between the feed-line and tapered slot. The rectangular shape tuning stub shows a good coupling with tapered shape slot proving a wider impedance matching for UWB application.

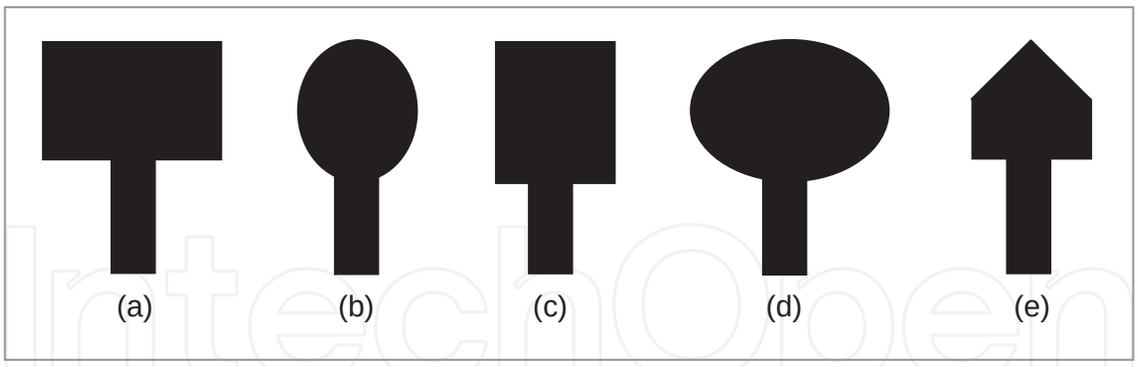

Figure 2. Different tuning stub shape (a) Rectangular (b) Circular, (c) Square, (d) Elliptical and (e) Tapered.

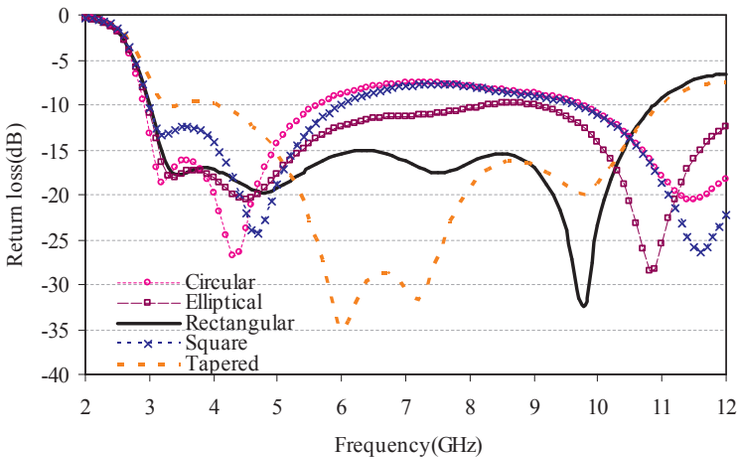

Figure 3. Simulated return loss curves for different tuning stub shape

3.2. Effect of slot shape

The wide-slot antenna is well-known to have wide impedance bandwidth though its operating bandwidth is limited due to the degradation of the radiation patterns at higher frequencies [7]. Through the numerical study on different slot shapes as shown in Figure 4, it is seen that currents flowing on the edge of the slot will increase the cross-polarization component in the *yz*-plane and cause the main beam to tilt away from the broadside direction in the *xz*-plane. Unlike the conventional wide-slot antenna proposed in [17], the slot in the ground plane of the proposed antenna with tapered shape is surrounded by ground strips of small width, which makes the antenna very compact. Moreover, introduction of the tapered slot instead of the rectangular slot changes the electric field distribution by reducing the longest current path and reducing the slot size. As a result, the impedance matching is much improved, especially at lower frequencies, resulting in overall enhancement of operating bandwidth as shown in Figure 5. It is also observed that high-frequency performance can also be

http://dx.doi.org/10.5772/51961

improved by employing tapered slot structure, and a tapered-shape slot matched with a rectangular tuning stub can produce wider bandwidth than with a circular, elliptical, and square-shaped slot.

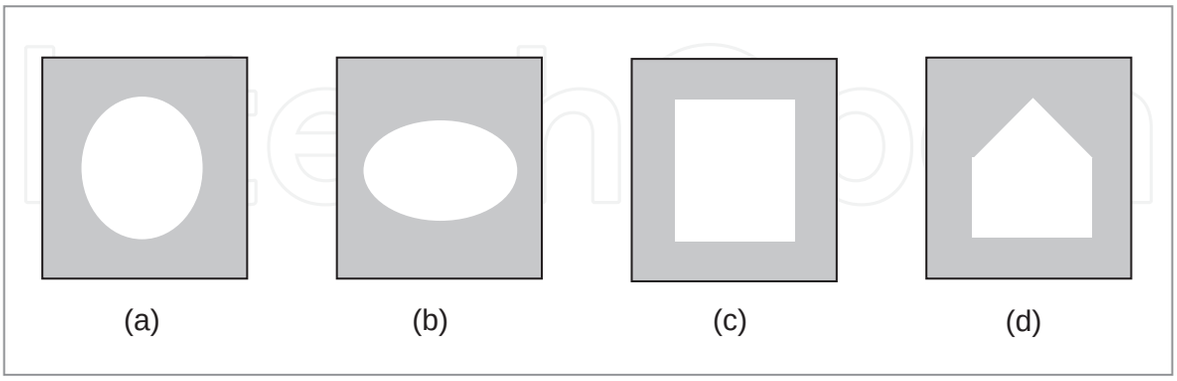

Figure 4. Different slot shape (a) Circular, (b) Elliptical, (c) Square and (d) Tapered.

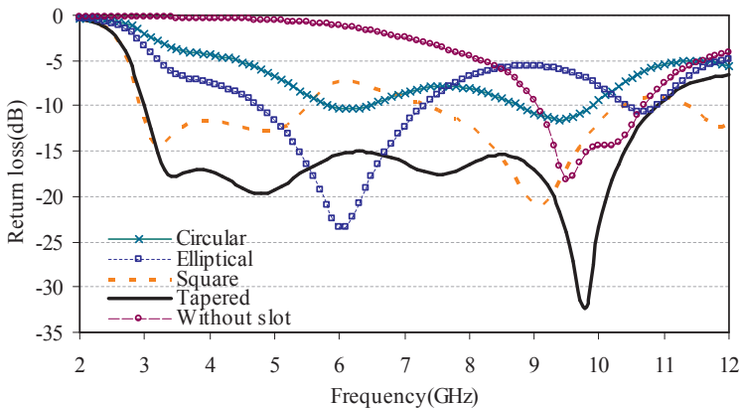

Figure 5. Simulated return loss curves for different tuning slot shape.

3.3. Effect of feed gap

The gap between the slot and the ground plane determines the matching between the feed line and slot antenna. The effect of feed gap on the impedance matching was investigated in [7] and [21]. It was found that by enhancing the coupling between the slot and microstrip feed line, good impedance matching can be obtained. An optimum value of the impedance bandwidth can be obtained for a certain optimum value of coupling. However, if the coupling increases further from this optimum value, the impedance matching becomes worse due to over-coupling. Figure 6 shows the simulated results of the proposed antenna for different feed gaps of -0.25, 0, 0.75 and 1.25 mm. It can be observed from the Figure that lower edge frequency of the operating band is highly dependent on the feed gap, while the feed

gap has a little effect on the upper edge frequencies. It is also observed that a feed gap of 0.75 mm can give the widest operating band with good return loss values. Table 1 is therefore represents a good summary of the optimized parameters of the proposed antenna for achieving the ultra-wide impedance bandwidth.

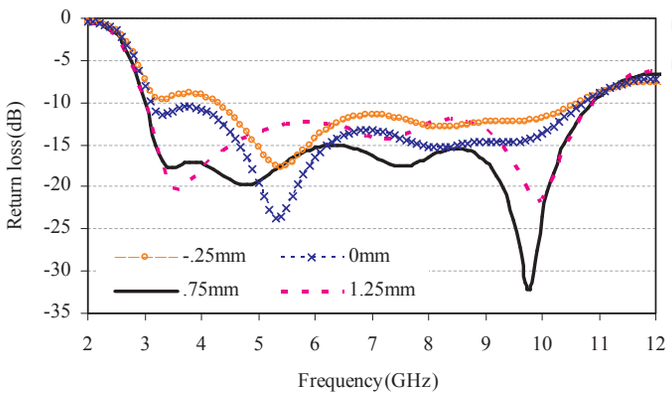

Figure 6. Simulated return loss curves for different feed gap.

Parameter	Value(mm)
W	22
L	24
W_1	2
L_1	10.75
w_2	11
L_2	7
W_3	18
w	13
l	7
w_f	3
α	90^0
h	0.75

Table 1. Optimized antenna parameters

http://dx.doi.org/10.5772/51961

4. Antenna performance and characteristics

A prototype of tapered shape slot antenna with optimal parameters tabulated in Table 1 is fabricated for experimental verification as shown in Figure 7. The antenna performance is measured in an anechoic chamber using Satimo's antenna measurement system and Agilent E8362C vector network analyzer.

4.1. Input impedance characteristics and current distribution

The measured and simulated return loss curves of the proposed antenna are depicted in Figure 8. It is seen that the proposed antenna exhibits a wideband performance from 3 to 11.2 GHz (115.5%) for -10 dB return loss value. The measured result agrees reasonably with the simulated one across the whole operating band. The disagreement between simulation and measurement is mainly due to the fabrication tolerance. It may also be due to the effect of the feeding cable as the antenna is small. Despite being physically small than the antenna proposed in [7, 13, 17, 20, 21], the antenna still achieved wide bandwidth to cover the entire ultra-wide frequency band.

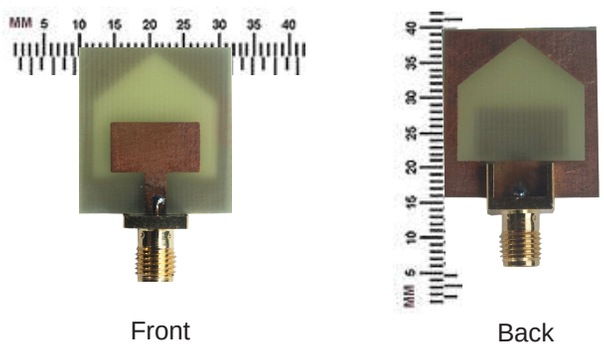

Figure 7. Photograph of the realized antenna.

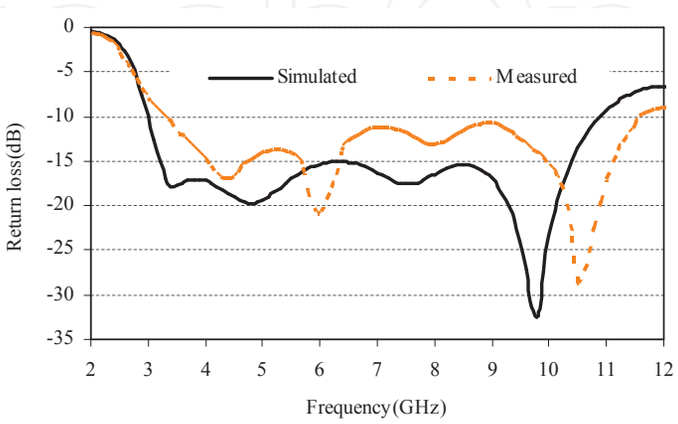

Figure 8. Simulated and measured return loss curves of the proposed antenna.

It is observed from the return loss curve that the proposed antenna is capable of supporting multiple resonances. The first resonance emerges at around 3.4 GHz, the second resonance at 6 GHz, third resonance at 8 GHz and fourth one at 10 GHz. The overlapping of these resonances, which are closely spaced over the spectrum leads to an ultra-wide operating band, which support the principle presented in [24].

The input impedance of proposed antenna is shown in Figure 9. Though there is variation in the frequency range from 5 - 8 GHz, it is seen in the Figure that the resistance is nearly flat and tends to 50 Ω values while the reactance is relatively constant at 0 Ω. Moreover, at these frequencies the measured phase of the input impedance is almost linear, which ensure that all the frequency components of the signal have the same delay leading to less pulse distortions. It is also seen that at the higher frequency end the resistance and reactance are getting away from 50 Ω and 0 Ω lines, respectively, i.e. the impedance matching is getting worse.

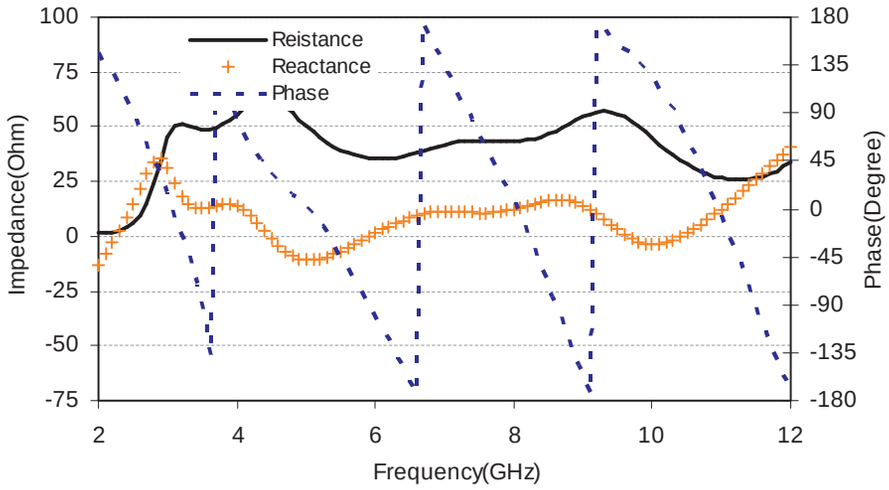

Figure 9. Input impedance and phase of the proposed slot antenna.

The return loss curve or the input impedance can only illustrate the antenna performance as a lumped load at the end of microstrip line [25]. The electromagnetic characteristics of the antenna can only be understood by examining the current distributions behavior at resonance frequencies. Simulated surface current distributions on the antenna close to the resonance frequencies are depicted in Figure 10. Figure 10(a) shows the current distribution at first resonance frequency of 3.4 GHz. The current pattern near the second resonance at around 6 GHz is shown in Figure 10(b), representing approximately a second order harmonic. Figure 10(c) present third order harmonic at 8 GHz. Figure 10(d) plots a more complicated current pattern at 10 GHz, corresponding to the fourth order harmonic. These current distributions is also support the principle that the overlapping of closely spaced resonances resulting in UWB characterization of the proposed antenna. At these four frequencies the resonances are clearly observed on the edges of both the tapered shape slot and rectangular tuning stub.

http://dx.doi.org/10.5772/51961

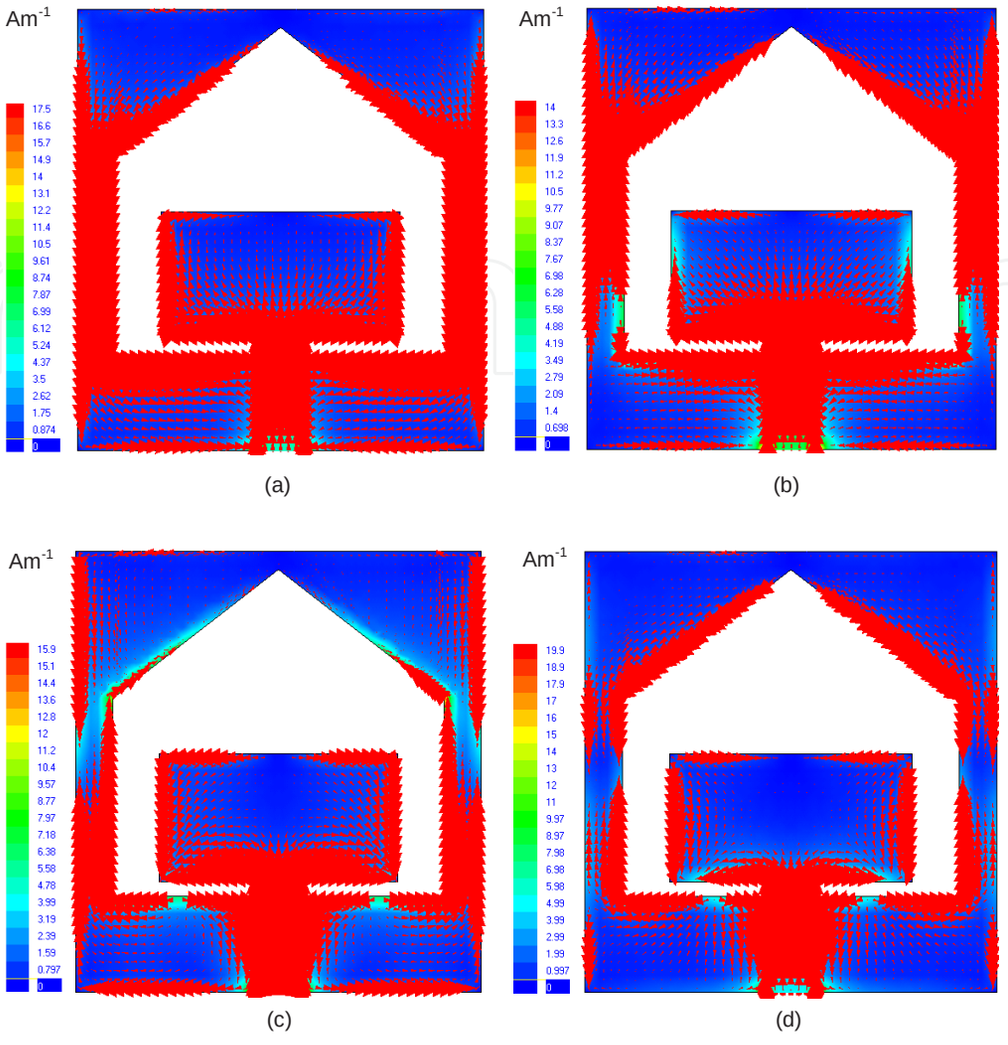

Figure 10. Simulated current distributions at (a) 3.4, (b) 6, (c) 8 and (d) 10 GHz.

4.2. Radiation characteristics

Satimo Starlab 0.6–18 GHz anechoic chamber at University of Hong Kong is used for the measurements of gain, total antenna efficiency, and radiation pattern [27]. This system uses the near-field measurement techniques that allow measurement of electric fields within the near-field of the antenna to calculate the equivalent far-field data of the antenna under test. The near-field of an antenna is the area close to the antenna, where the electric charge and electromagnetic induction effects occur. These effects fade out far more rapidly with increasing distance from the antenna (proportional to the cube of the distance) than the radiated electromagnetic far-field that fades out proportional to the distance. Near-field effects become negligible more than a few wavelengths away from the antenna. Once the near-field data have been measured, a Fourier transformation is used to calculate the equivalent far-field data. The antenna, mounted on the test board, is positioned in the center of a circular "arch" that contains 16 separate measurement probes. These probes are spaced equally apart

along the circular surface. The antenna is rotated horizontally through 360°, and the combination of this rotation and the array of probes allows a full 3D scan of the antenna to be carried out, allowing full 3D radiation patterns to be measured, plotted, and analyzed. Information about antenna gain and efficiency can then be calculated from the far-field radiation pattern data. A coaxial cable was incorporated in the measurement system and the system was calibrated.

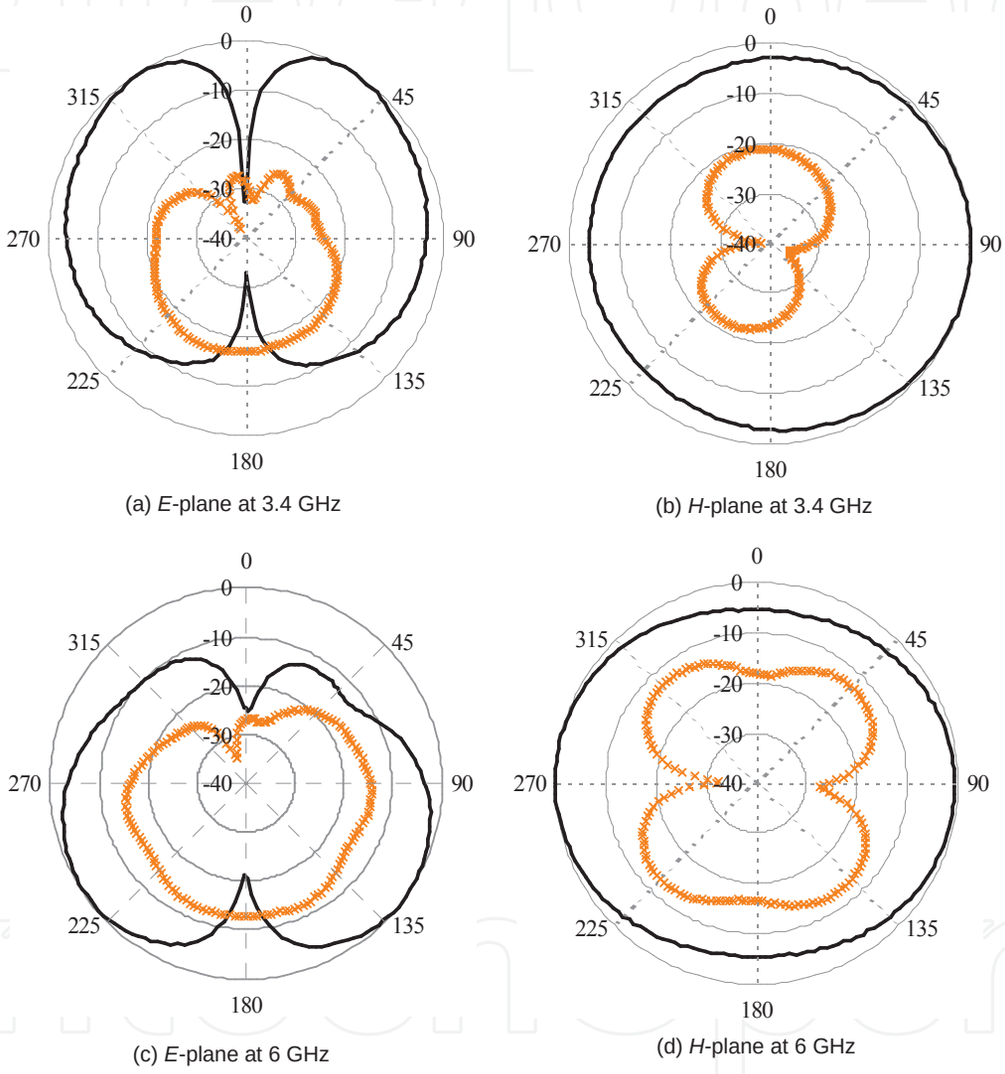

Figure 11. Measured radiation patterns at 3.4 GHz and 6 GHz [solid line: co-polarization, crossed line: cross-polarization].

Figures 11 and 12 show the measured 2D radiation patterns in two principal planes-namely, the *E*-(*xz*) and *H*-(*xy*) planes for four resonant frequencies of 3.4, 6, 8 and 10 GHz. It can be observed that at lower frequencies the antenna exhibit an omni-directional radiation patterns for *H*-plane and donut shape for *E*-plane with low cross-polarization field and patterns are about the same as that of a typical monopole antenna. As the frequency increases, higher

http://dx.doi.org/10.5772/51961

order harmonic introduced to patterns and both *H*- and *E*-plane become more directional but still retain omni-directionality. Polarization purity can only be seen at low frequency region where the cross-to-co polarization ratio is around -20 dB, in contrast to higher frequencies, where the cross-polarization is dominant especially in *H*-plane. The slight asymmetry observed at higher frequencies in both in *H* -and *E* -plane may be due to the fact that microstrip feed line itself act as a radiator.

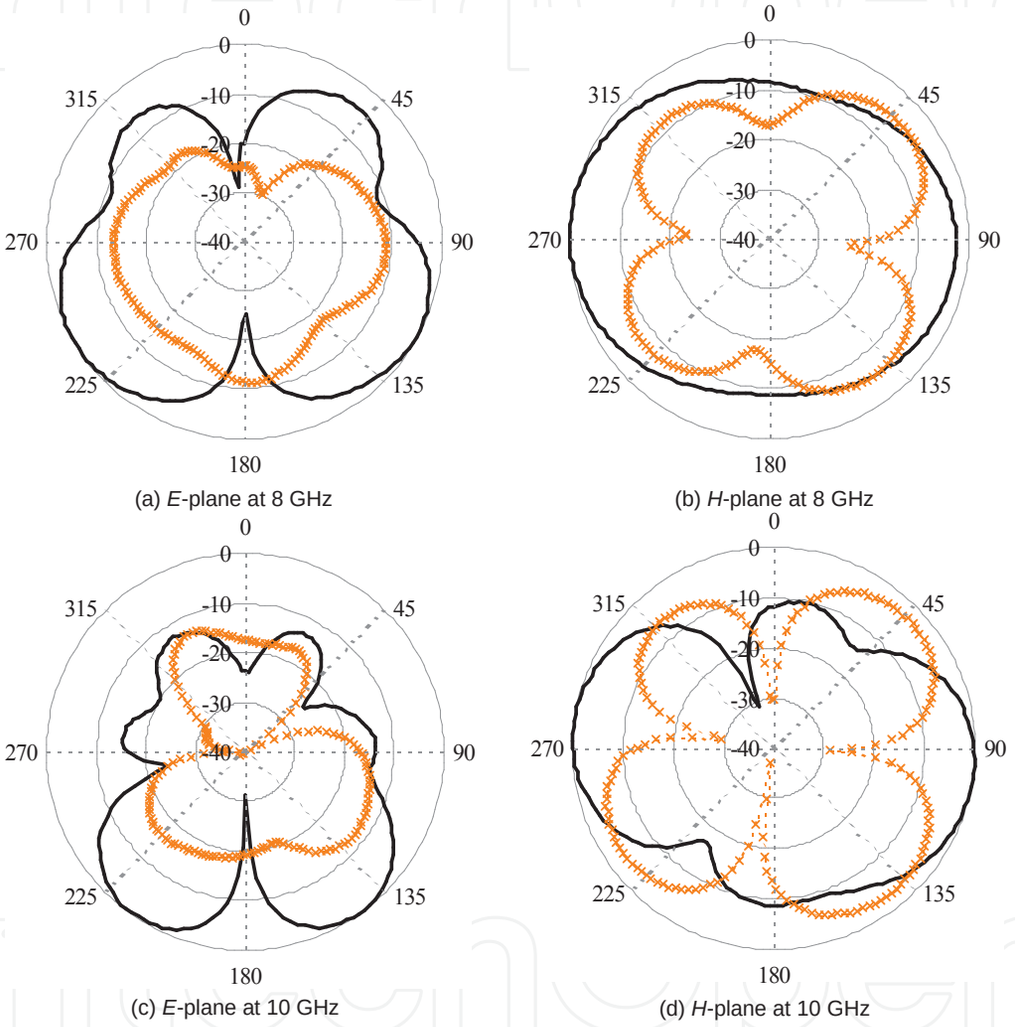

Figure 12. Measured radiation patterns at 8 GHz and 10 GHz [solid line: co-polarization, crossed line: cross-polarization].

Figure 13 depict the measured 3D radiation patterns at 3.4 and 8 GHz. In the patterns the red color indicates the stronger radiated *E*-field and the blue is the weakest ones. At low frequency of 3.4 GHz, the radiation patterns are almost omni-directional similar to a typical monopole antenna. The radiation is slightly weak in *z*-direction. At the higher frequency of 8 GHz, the radiation becomes slightly directional with a null in the *z*-direction due to higher order harmonics. The 3D omni-directional radiation patterns of the proposed antenna make

it suitable for being used in different wireless communications especially in mobile communication.

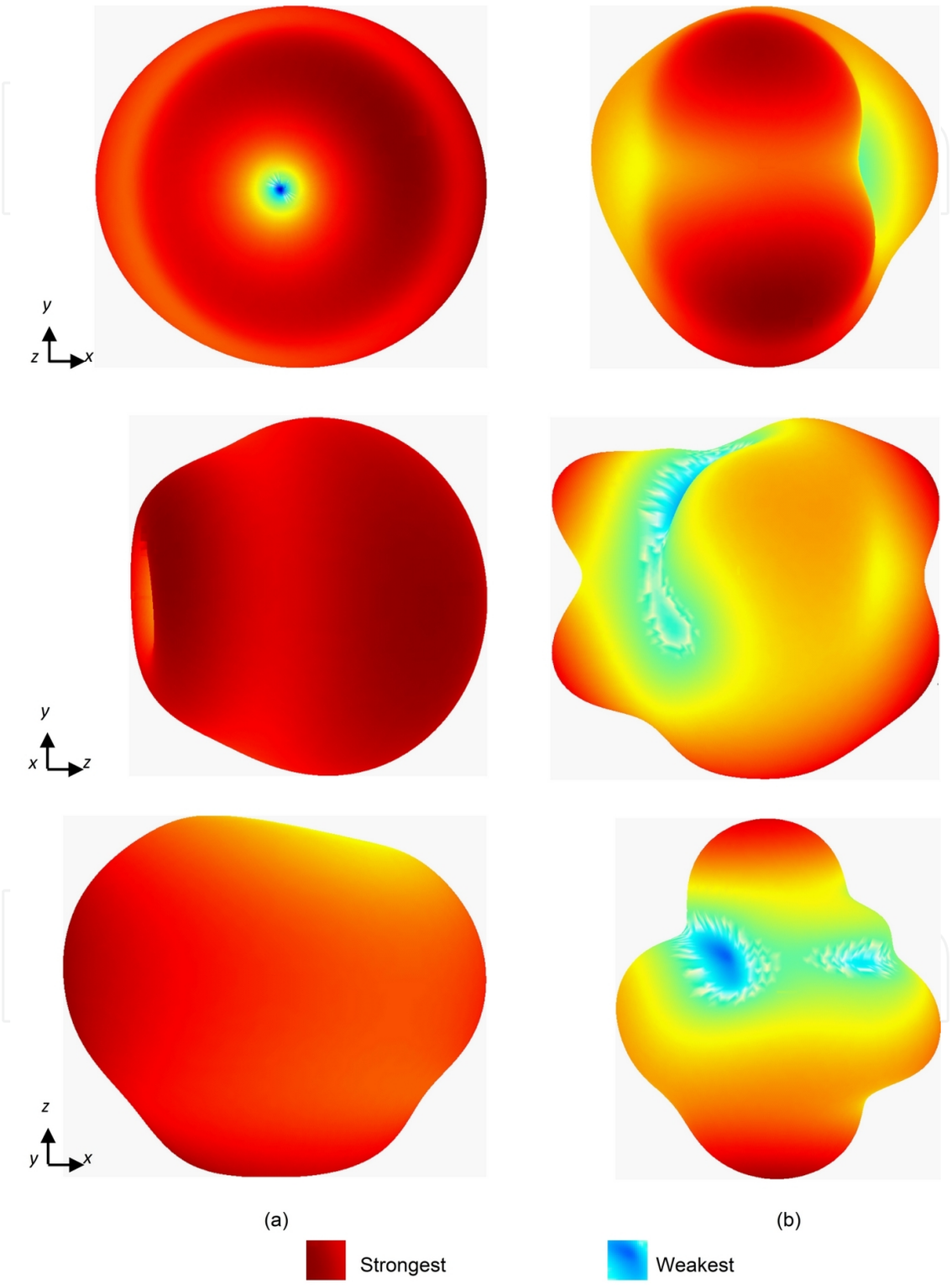

Figure 13. Measured 3D radiation pattern in *xy*, *yz* and *xz*-planes at (a) 3.4 and (b) 8 GHz.

4.3. Gain and radiation efficiency

The measured peak gain of the proposed slot antenna is shown in Figure 14. From the Figure, it can be seen that the proposed antenna achieves an average peak gain of 3.81 dBi. The maximum realized gain is 5.4 dBi at 9.8 GHz, where the radiation patterns become slight directional.

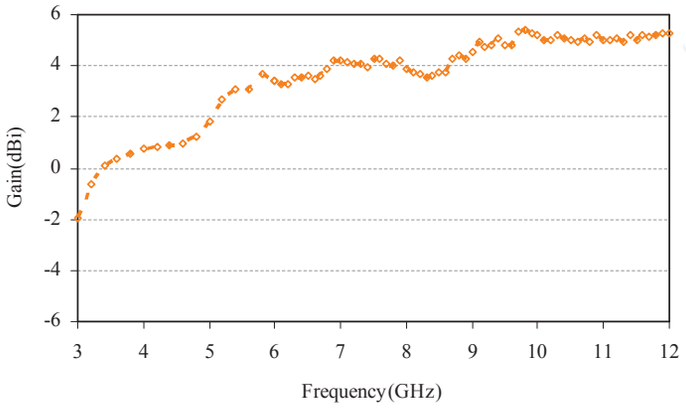

Figure 14. Measured peak antenna gain.

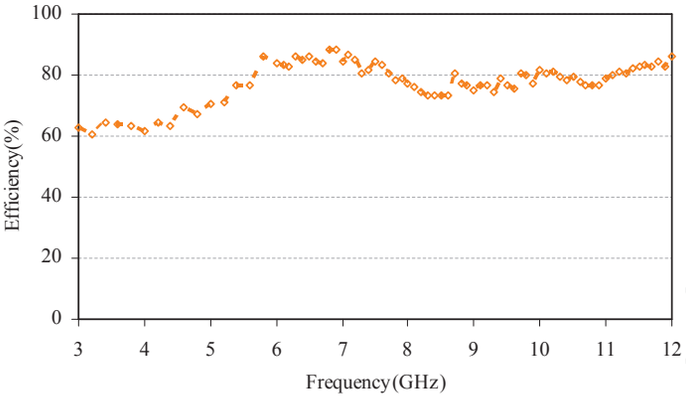

Figure 15. Measured radiation efficiency.

The realized radiation efficiency of the proposed antenna is shown in Figure 15. It is seen that the fabricated antenna achieves an average radiation efficiency of 77.9% and the maximum efficiency is 88.2%. Despite of fluctuations observed in the curves due to wider bandwidth, the proposed slot antenna achieves good gain and radiation efficiency with a compact profile in comparison with the other reported microstrip line fed planar antennas and is similar to those proposed in [17] and [26].

5. Time domain behavior

Since UWB systems directly transmit narrow pulses rather than continuous wave, the time domain performances of the UWB antenna is very crucial. A good time domain performances is a primary requirement of UWB antenna. The antenna features can be optimized to avoid undesired pulse distortions. For a transmitting/receiving antenna system as shown in Fig. 16(a), the transfer function (S_{21} parameter) is required to have flat magnitude and linear phase response over the operating band to minimize the distortions in the received signal waveform and is defined as [28-30]

$$T(\theta,\varphi,\omega) = \frac{\sqrt{\eta_0 Z_0}}{Z_0 + Z_A(\omega)} \vec{h}_{eff}(\theta,\varphi,\omega) \tag{1}$$

where $\vec{h}_{eff}$ is the complex vector effective height and $Z_A(\omega)$is the antenna input impedance. In terms of this transfer function the port-to-port S_{21} between transmitting and receiving antennas is

$$S_{21}(\omega) = j\omega \vec{T}_{TX}(\omega) \bullet \vec{T}_{RX}(\omega) \frac{e^{-jkR}}{2\pi R C_0} \tag{2}$$

where $\omega=2\pi f$, f is the operating frequency, C_0 is the velocity of light, (θ, φ) is the orientation and $\vec{T}_{TX}$ and $\vec{T}_{RX}$ are the transfer functions of the transmitting and receiving antennas respectively. If S_{21} is measured using two identical antennas, for single polarization, the transfer can be calculated as

$$T(\omega) = \sqrt{\left(\frac{2\pi R c_0}{j\omega} S_{21}(\omega) e^{j\omega R / C_0} \right)} \tag{3}$$

The distance, R is to be derived from the S_{21} data itself.

The group delay is defined as the negative derivative of the phase response with respect to frequency and usually used to evaluate the phase response of the transfer function. The group delay gives an indication of the time delay of an impulse signal at different frequencies. Ideally, when the phase response is strictly linear, the group delay variation is zero. The transfer functions and group delay between a pair of proposed antennas had been measured inside an anechoic chamber with dimension of 4 m × 4 m × 8 m using Satimo's StarLab antenna measuring equipment. Since UWB technology employed in short range communication systems, in the measurements the transmitting and receiving antennas are placed face-to face at distance 0.5 m apart as illustrates in Figure 16. The measurements were taken at different azimuth angle in *xz*-plane.

http://dx.doi.org/10.5772/51961

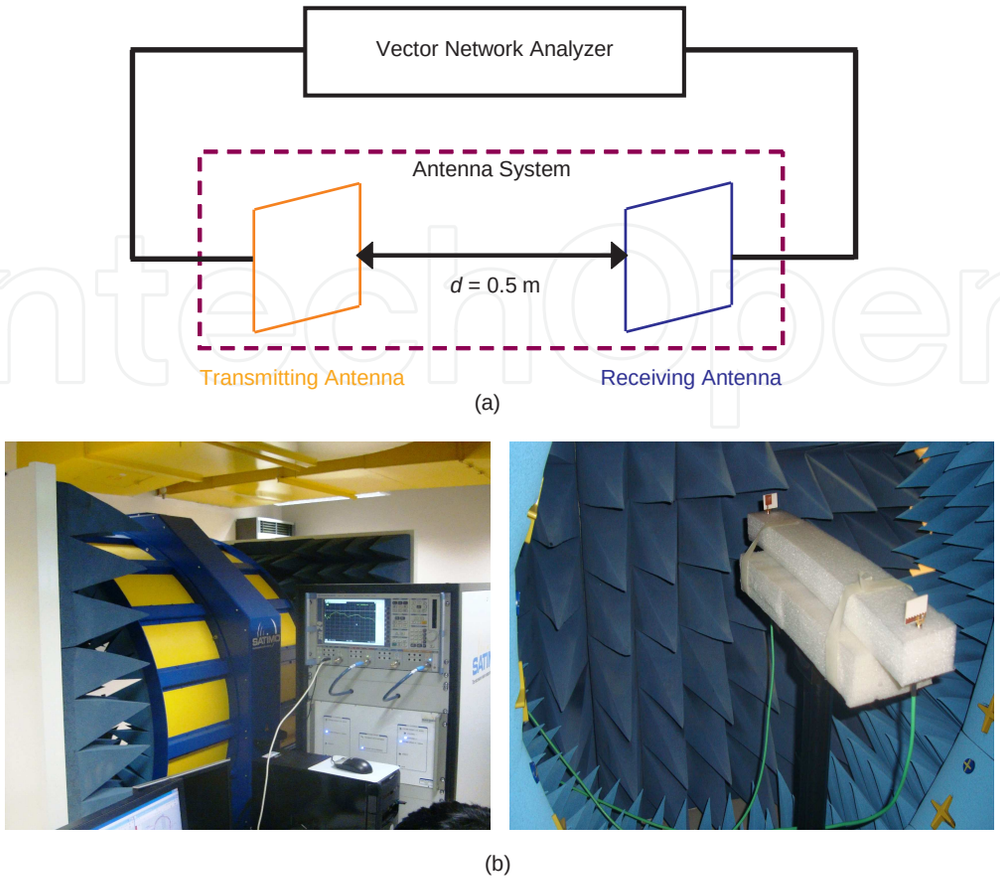

Figure 16. Setup for transfer function and group delay measurement (a) schematic diagram and (b) in anechoic chamber.

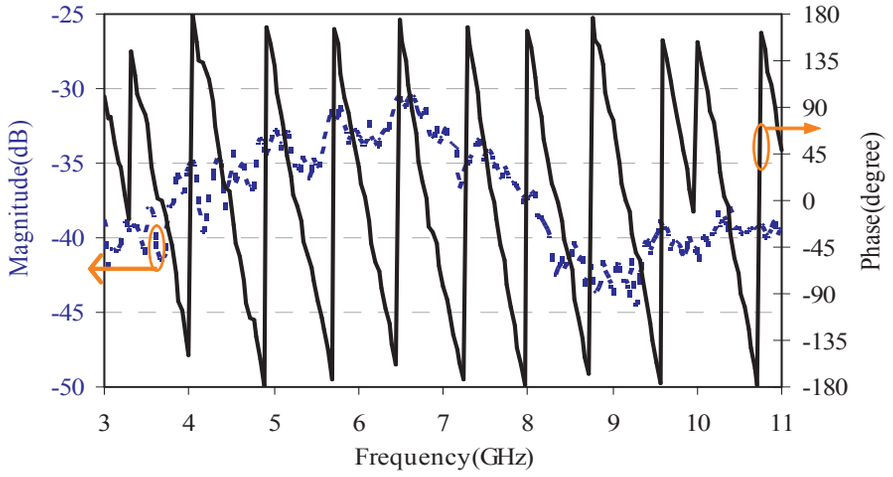

Figure 17. Magnitude and phase of the measured transfer function.

The magnitude and phase of the measured transfer function of the proposed antenna are shown in Figure 17. It is observed that the magnitudes of the transfer function are relatively smooth over the whole UWB frequency range and the variation is less than 10 dB. Linear phase response is also observed within the frequency range from 3 - 10 GHz as depicted in Figure 17. The measured group delay as shown in Figure 18 demonstrates relatively constant responses over the entire UWB frequency band. The average variation in the group delay is less than 1.3 ns, which corresponds very well to the phase of the transfer functions. This small variation in transfer function indicates that the proposed antenna does not distort the phase of the transmitted/received signals, which is a primary requirement of UWB applications.

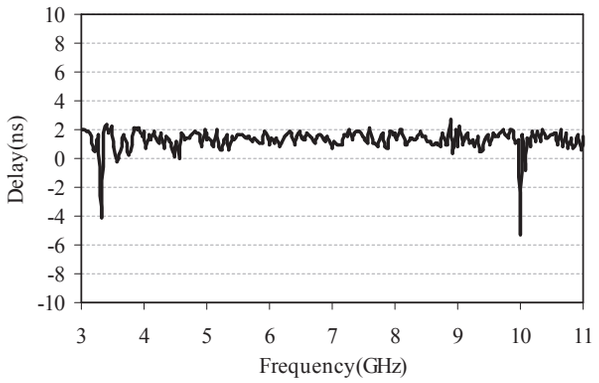

Figure 18. Measured group delay of the proposed antenna.

6. Conclusion

The design of a compact printed wide slot antenna has been proposed and implemented for ultra-wideband applications. The proposed antenna consist of a tapered shape slot and rectangular tuning stub, and fabricated onto a 22 mm × 24 mm× 1.6 mm size FR4 dielectric substrate. The measured results show that the proposed antenna achieves good impedance matching constant gain, stable radiation patterns over an operating bandwidth of 3 to 11.2 GHz (115.5%) to cover the entire UWB. The stable radiation pattern with a maximum gain of 5.4 dBi and good time domain behaviors makes the proposed antenna a suitable candidate for practical UWB applications.

Acknowledgements

This work is funded by Universiti Kebangsaan Malaysia under the grant DIP-2012-06. The authors would like to thank Associate Professor S. W. Cheung for allowing using the SATI-

MO's StarLab antenna measurement equipment of Department of Electrical and Electronic Engineering, University of Hong Kong.

Author details

Rezaul Azim[1] and Mohammad Tariqul Islam[1,2]

1 Institute of Space Science (ANGKASA), Universiti Kebangsaan Malaysia, Malaysia

2 Department of Physics, University of Chittagong, Bangladesh

References

[1] Allen, B., Dohler, M., Okon, E., Malik, W., Brown, A., Edwards, D. *Ultra-wideband Antennas and Propagation for Communications, Radar and Imaging*. New York: John Wiley & Sons, Ltd. (2006).

[2] Chen, C. C., Rao, K. R., Lee, R. A New Ultrawide-bandwidth Dielectric-rod Antenna for Ground-Penetrating Radar Application. *IEEE Transactions on Antennas & Propagation*, 51, 371-377(2003).

[3] Chang, L. T., Burnside, W. D. An Ultrawide-Bandwidth Tapered Resistive TEM Horn Antenna. *IEEE Transactions on Antennas & Propagation*, 48, 1848–1857(2000).

[4] Shakib, M. N., Islam, M. T., Misran, N. Stacked Patch Antenna with Folded Patch Feed for Ultra-wideband Application. *IET Microwave Antennas & Propagation*, 4, 1456–1461(2010).

[5] Azim, R., Islam, M. T., Misran, N., Cheung, S. W., Yamada, Y. Planar UWB Antenna with Multi-Slotted Ground Plane. *Microwave & Optical Technology Letters*, 53, 966-968 (2011).

[6] Schantz, H. G. UWB Magnetic Antennas. *Proceedings of the IEEE Antennas & Propagation Society International Symposium*, 22-27 June (2003), Columbus, Ohio, USA, 604 - 607.

[7] Liu, Y. F., Lan, K. L., Xue, Q., Chan, C. H. Experimental Studies of Printed Wide-slot Antenna for Wide-band Applications. *IEEE Antennas & Wireless Propagation Letters*, 3, 273 – 275 (2004).

[8] Qu, S. W., Ruan, C., Wang, B. Z. Bandwidth Enhancement of Wide-slot Antenna fed by CPW and Microstrip Line. *IEEE Antennas & Wireless Propagation Letters*, 5, 15 – 17 (2006).

[9] Latif, S. I., Shafai, L., Sharma, S. K. Bandwidth Enhancement and Size Reduction of Microstrip Slot Antenna. *IEEE Transactions on Antennas & Propagation*, 53, 994 – 1003 (2005).

[10] Lui, W. J., Cheng, C. H., Zhu, H. B. Experimental Investigation on Novel Tapered Microstrip Slot Antenna for Ultra-wideband Applications. *IET Microwave & Antennas Propagation*, 1, 480 – 487 (2007).

[11] Qing, X., Chen, Z. N. Compact Coplanar Waveguide-fed Ultra-wideband Monopole-like Slot Antenna. *IET Microwave & Antennas Propagation*, 3, 889 – 898 (2009).

[12] Chang, D. C., Liu, J. C., Liu, M. Y. Improved U-Shaped Stub Rectangular Slot Antenna with Tuning Pad for UWB Applications. *Electronics Letters*, 41, 1095-1097 (2005).

[13] Jan, J. Y., Kao, J. C. Novel Printed Wide-Band Rhombus-like Slot Antenna with an Offset Microstrip-fed Line. *IEEE Antennas & Wireless Propagation Letters*, 6, 249 – 251 (2007).

[14] Sze, J. Y., Chang, C. C. Circularly Polarized Square Slot Antenna with a Pair of Inverted-L Grounded Strips. *IEEE Antennas & Wireless Propagation Letters*, 7, 149-151 (2008).

[15] Gopikrishna, M., Krishna, D. D., Anandan, C. K., Mohanan, P., Vasudevan, K. P. Design of a Compact Semi-Elliptic Monopole Slot Antenna for UWB Systems. *IEEE Transactions on Antennas & Propagation*, 57, 1834-1837(2009).

[16] Chair, R., Kishk, A. A., Lee, K. F., Smith, C. E. Microstrip Line and CPW Fed Ultra Wideband Slot Antennas with U-Shaped Tuning Stub and Reflector. *Progress In Electromagnetics Research*, 56, 163-182 (2006).

[17] Chen, H. D. Broadband CPW-fed Square Slot Antennas with a Widened Tuning Stub. *IEEE Transactions on Antennas & Propagation*, 51, 1982 – 1986 (2003).

[18] Chiou, J. Y., Sze, J. Y., Wong, K. L. A Broad-band CPW-fed Strip-loaded Square Slot Antenna. *IEEE Transactions on Antennas & Propagation*, 51, 719-721(2003).

[19] Liu, Y. F., Lan, K. L., Xue, Q., Chan, C. H. Experimental Studies of Printed Wide-slot Antenna for Wide-band Applications. *IEEE Antennas & Wireless Propagation Letters*, 3, 273 – 275 (2004).

[20] Jan, J. Y., Su, J. W. Bandwidth Enhancement of a Printed Wide-slot Antenna with a Rotated Slot. *IEEE Transactions on Antennas & Propagation*, 53, 2111 – 2114 (2005).

[21] Dastranj, A., Imani, A., Moghaddasi, M. N. Printed Wide-slot Antenna for wideband applications. *IEEE Transactions on Antennas & Propagation*, 56, 3097 – 3102 (2008).

[22] Ma, T. G., Tseng, C. H. An Ultrawideband Coplanar Waveguide-fed Tapered Ring Slot Antenna. *IEEE Transactions on Antennas & Propagation*, 54, 1105-1110 (2006).

[23] IE3D Version 12. Zeland Software Inc;(2010).

[24] Liang, J., Guo, L., Chiau, C. C., Chen, X., Parini, C. G. Study of CPW-fed Circular Disc Monopole Antenna for Ultra-wideband Applications. *IEE Proceedings of Microwaves, Antennas & Propagation*, 152, 520–526 (2005).

[25] Liang, J., Chiau, C. C., Chen, X., Parini, C. G. Study of a Printed Circular Disc Monopole Antenna for UWB Systems. *IEEE Transactions on Antennas & Propagation*, 53, 3500–3504 (2005).

[26] Sze, J. Y., Wong, K. L. Bandwidth Enhancement of a Microstrip-line-fed Printed Wide-slot. *IEEE Transactions on Antennas & Propagation*, 49, 1020 – 1024 (2001).

[27] Foged, L. J., Giacomini, A. Wide Band Dual Polarized Probes for Near and Far Field Measurement Systems. *Proceedings of the IEEE Antennas & Propagation Society International Symposium*, 5-11 July (2008), CA, USA, 5-11.

[28] Scheers, B., Acheroy, M., Vorst, A. V. Time Domain Simulation and Characterisation of TEM Horns using Normalised Impulse Response. *IEE Proceedings Microwaves, Antennas & Propagation*, 147, 463-468 (2000).

[29] Qing, X., Chen, Z. Transfer Functions Measurements of UWB Antenna. *Proceedings of the IEEE Antennas & Propagation Society International Symposium*, 20-25 June (2004), CA, USA, 2532-2535.

[30] Guo, L., Liang, L., Chiau, C. C., Chen, X., Parini, C. G., Yu, J. Performance of Ultra-wideband Disc Monopoles in Time Domain. *IET Microwaves, Antennas & Propagation*, 1, 955-959 (2007).

IntechOpen